Electrospinning of Neat and Laponite-Filled Aqueous Poly(ethylene oxide) Solutions

VIKRAM K. DAGA, MATTHEW E. HELGESON, NORMAN J. WAGNER

Center for Molecular and Engineering Thermodynamics, Department of Chemical Engineering, University of Delaware, Newark, Delaware 19716

Received 23 August 2005; revised 3 February 2006; accepted 8 February 2006
DOI: 10.1002/polb.20784
Published online in Wiley InterScience (www.interscience.wiley.com).

ABSTRACT: Electrospinning is reported for viscoelastic aqueous solutions of poly(ethylene oxide) (PEO) and with added nanoclay (laponite). A weak correlation between fiber diameter and the spinning solution's zero-shear viscosity is observed and compared with previous work reported by McKee et al. (McKee et al., Macromolecules 2004, 37, 1760). A new analysis of electrospinning results for PEO indicates a universal correlation between fiber diameter and solution properties that does not include shear viscosity as a primary variable. The addition of laponite nanoclay to the PEO solutions, which has been previously shown to result in rheologically simple solutions, leads to different fiber morphologies for the same shear viscosity in contradiction with reports for titania particles (Drew et al., J Macromol Sci Part A: Pure Appl Chem 2003, 40, 1415). The research identifies additional physicochemical properties that are important in determining electrospun fiber morphology. ©2006 Wiley Periodicals, Inc. J Polym Sci Part B: Polym Phys 44: 1608–1617, 2006

Keywords: electrospinning; laponite; polymer–colloid mixtures; polymer–clay composites; viscoelasticity; viscosity; master curve

INTRODUCTION

Electrospinning has received significant research interest because it is a rapid, direct, and relatively simple method to produce polymeric nanofibers[1–6] from which a variety of potential novel applications are emerging.[7–16] Electrospinning results in nonwoven, porous mats of fibers of diameter of a few nanometers to a few micrometers. The fiber morphology depends on the rheological and electrical properties of the solutions being spun and the operating conditions, as demonstrated for several polymer solutions.[17–21] Various instabilities can occur in the jet, such as "whipping"[3,18,22–24] and "splaying."[18,24] In addition, a capillary instability can lead to the formation of beads for less viscous spinning solutions.[25] A varicose instability has also been shown to produce beaded fibers.[2,3] The electrospun jet dries rapidly but may reach the collector in a partially or completely dried state depending upon the volatility of the solvent used, which can lead to coalescence of fibers to produce a mechanically connected, nonwoven mat.

Successful electrospinning occurs in an identifiable range of electrical and rheological properties of the polymer solution or melt[3,22] and processing conditions. For example, the spinning solution must be sufficiently viscous such that fibers can be drawn without breaking up into droplets (i.e. electrospraying). Shenoy et al. showed[26] that a polymer solution must be above a critical chain entanglement density to form continuous fibers, a result that has been prevalent for many different polymer systems.[25,27,28]

Correspondence to: N. J. Wagner (E-mail: wagner@che.udel.edu)

Journal of Polymer Science: Part B: Polymer Physics, Vol. 44, 1608–1617 (2006)

Recently, nanoparticles have been incorporated into the spinning solutions to yield composite fiber mats with potentially enhanced or new physical properties.[29,30–32] Electrospinning investigations of aqueous poly(ethylene oxide) (PEO) solutions by Drew et al.[29] suggest that the addition of titanium oxide particles also enables electrospinning at lower polymer concentrations than that normally possible. Particle addition leads to similar fiber diameters when the spinning solutions have comparable shear viscosities. However, the incorporation of nanoparticles into polymer solutions results in additional complications to the electrospinning process, and whether this observation is general for many polymer–nanoparticle composite systems is not well understood.

There is significant interest in quantifying the relationships connecting the resultant fiber mat properties, such as fiber diameter and morphology, to the solution's rheology, electrical properties, surface tension, and the process variables. For example, McKee et al.[27] correlated the final diameter of polyester fibers and the spinning solution's zero-shear viscosity, $D = 13{,}000(\eta_0)^{0.8}$ where D is expressed in nm and η_0 in Pa s. In addition, it was argued that the viscosity dependence of the fiber diameter was due to the influence of polymer chain entanglements on the rheology of the solutions, and thus fiber diameter also correlated well with the polymer concentration scaled by the critical concentration for entanglements, c_e. However, subsequent work by McKee et al.[28] showed that for solutions of polymers with associative interactions (such as hydrogen bonding), the fiber diameter increases more strongly with polymer concentration than expected for nonassociative polymers.

Alternatively, Fridrikh et al.[20] presented an analytical model for prediction of fiber diameter arising from a force balance between electrostatics, surface forces, and inertia due to "whipping" of the electrospinning jet. However, the model contains parameters that are difficult to measure experimentally (i.e. the "radius of whipping) and is shown only to hold for polymer solutions of sufficient conductivity. Overall, it is unclear from the previous work whether correlations of fiber diameter with solution rheology or electrostatics alone are sufficient to fully predict electrospinning behavior. Again, such correlations are system-specific at best, and whether similar quantitative relationships hold for ultimate fiber morphology in the presence of nanoparticles has not been established.

The goals of the work reported here are to determine if the correlation between zero shear viscosity and electrospun fiber diameter and morphology also holds for aqueous polymer solutions, and whether this can be extended to the electrospinning of solutions containing dispersed nanoparticles. In contrast to the polyester solutions examined by McKee et al.,[27] here we study model, viscoelastic, aqueous solutions of PEO.[33–37] In addition, the solvent used here (water) is less volatile than the 70/30 (w/w) mixture of chloroform/dimethyl formamide used by McKee et al.,[27] which may also be a factor in setting fiber morphology. Finally, we exploit the established rheological simplicity of the model system of aqueous PEO–laponite[37] to examine the influence of the addition of nanoclay on the electrospun fiber properties.

EXPERIMENTAL

Previous studies[37] of a model system of laponite (a synthetic nanoclay) dispersed in aqueous PEO solutions demonstrated that the linear viscoelasticity of neat and laponite-filled aqueous PEO solutions can be superimposed in the form of a master rheological curve. The concentration of these solutions and mixtures are shown in Tables 1 and 2 and the same sample names are used herein to facilitate comparison. The linear viscoelasticity of aqueous PEO solutions (PW solutions) and laponite-filled aqueous PEO solutions (PWL mixtures) were reduced to a single master curve by time–concentration superposition, as shown in Figure 1. Preparation of the samples is described in detail in the aforementioned reference and is summarized below.

PEO (Scientific Polymer Products, Inc.) with reported nominal $M_w = 9 \times 10^5$ g/mol, laponite RD (Southern Clay Products), and deionized

Table 1. Composition of Electrospun Aqueous PEO Solutions

Solution	PEO (wt %)
PW3	2.52
PW5	3.74
PW8	4.50
PW10	5.50
PW12	6.50

Table 2. Composition of Electrospun Laponite (L)-Filled Aqueous PEO (P) Solutions in Water (W)

Mixture	Base Solution	Group	P (wt %)	L (wt %)	$100P/(P + W)$	$100L/(L + P)$
PWL1	PW3	1	2.49	0.94	2.51	27.31
PWL2	PW5	2	3.71	0.66	3.73	15.09
PWL3	PW8	3	4.48	0.49	4.50	9.79
PWL4	PW10	4	5.49	0.26	5.50	4.48
PWL5	PW3	1	2.48	1.52	2.52	38.00
PWL6	PW5	2	3.69	1.18	3.74	24.28
PWL7	PW8	3	4.45	0.97	4.50	17.96
PWL8	PW10	4	5.46	0.70	5.50	11.33
PWL9	PW12	5	6.47	0.42	6.50	6.10

water with a resistivity of 18.3 MΩ cm were used as supplied. PEO (6.62 and 8.0 wt %) was added to deionized water in plastic bottles and sealed. The bottles were shaken vigorously to completely disperse the PEO. Three days were allowed for the complete dissolution of PEO in water during which the solutions, henceforth referred to as PW solutions, were placed on a rotating mixer for gentle mixing. The aqueous PEO solutions of lower concentrations were prepared by diluting either of the two stocks with an additional amount of deionized water, after which, the diluted samples were mixed for a day. Laponite (1.5 and 2.2 wt %) was added to deionized water and shaken vigorously for a few minutes and then sonicated for ~30 min using a probe sonicator with simultaneous mixing using a magnetic stirrer bar. Laponite dispersions, henceforth referred to as PWL mixtures, were used within 2 h of sonication to prevent aging.

The PWL mixtures of desired concentrations were prepared in glass vials from stock solutions

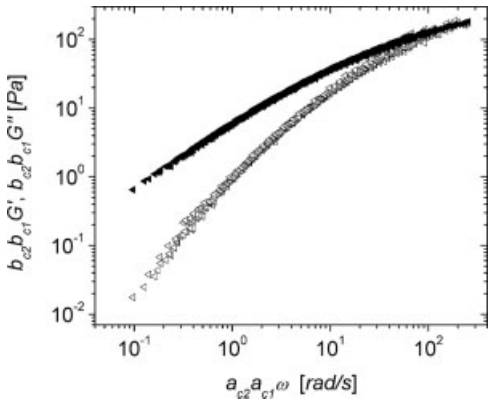

Figure 1. Complete time–concentration superposition master curve of PW and PWL mixtures at 25 °C in with reference to PW10. The shift factors and explanation of the data is described in detail in Daga and Wagner.[37]

of PEO and laponite dispersions by mixing 6.62 wt % PEO solution with 1.5 wt % laponite dispersion and mixing 8 wt % PEO solution with 2.2 wt % laponite dispersion in different weight ratios. Figure 2 shows the organization of the solutions into groups on a ternary diagram. Each group consists of varying laponite concentration in solutions with fixed PEO–water composition. The PWL samples were stirred briefly and then mixed on a vibrating mixer for a minimum of ~24 h. The PWL mixtures were optically clearer than neat PW solutions but some of the mixtures with higher laponite concentrations formed colorless gel-like agglomerates that settled with time. These agglomerates are characteristic of this system.[38] Once sufficient mixing was allowed, the conductivity of the PW and PWL solutions was measured using a Malvern Zetasizer in zeta potential measurement mode.

All electrospinning experiments were carried on sheared PWL mixtures within 3 days of their preparation to avoid any effect of sample aging. Electrospinning experiments were performed using a device described previously.[21] A DC voltage of 20 kV, a collector to tip distance of 13 cm and a flow rate of 3 mL/h was used for all experiments. Fiber mats were collected on aluminum substrate (foil) and SEM (JEOL JSM 6335F) digital micrographs were obtained and analyzed using Adobe Photoshop software to obtain the fiber diameter distributions.

RESULTS AND DISCUSSION

SEM micrographs of electrospun fibers from solutions listed in Table 1 are shown in Figure 3, organized according to groups. Solution PW3, with a PEO concentration slightly below the transition to the concentrated regime (c^{**}),[37] exhibited bead formation along the axis of the

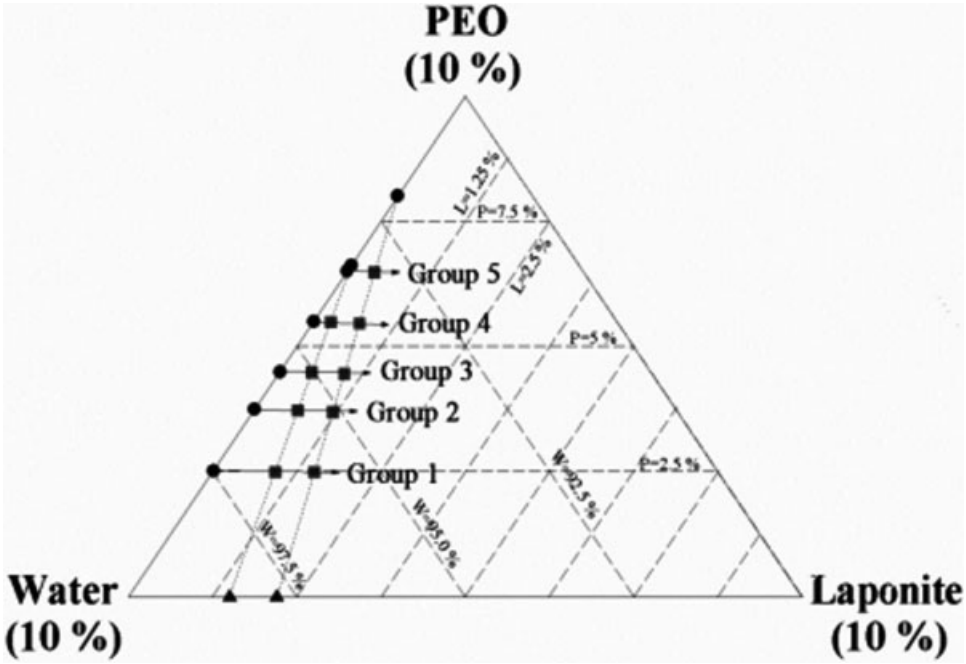

Figure 2. Concentration map of neat and laponite-filled aqueous PEO solutions prepared for electrospinning: circles, triangles, and squares represent the PEO solutions, laponite dispersions, and laponite-filled PEO solutions, respectively. Solutions that lie on an arrow represent members of a group.

fibers. The addition of laponite reduced beading, in qualitative agreement with the observations of Drew et al.[29] All other samples were in the concentrated regime and formed fibers without beading. Laponite addition at higher polymer concentration leads to a broader distribution in fiber diameters.

The average (number) diameter of the PW and PWL electrospun fibers and the zero shear viscosity[37] of the spun solutions are shown in Table 3. Figure 4 shows that the average diameter of PEO fibers correlates with the zero shear viscosity as (where D is in nm and η_0 in Pa-s),

$$D = (127 \pm 6)\eta_0^{(0.16 \pm 0.02)}$$

Although this result is similar to a previous report for polyester solutions by McKee et al.,[27] the power law dependence of fiber diameter on viscosity is much weaker. The former correlation is also shown in Figure 4 for comparison, demonstrating that such correlations are not transferable across materials and electrospinning parameters.

The average diameter of the PWL electrospun fibers and the zero shear viscosity[37] and conductivity of the PWL mixtures are shown in Table 3 and plotted in Figure 5 along with the standard deviation. Large variation in the measured fiber diameters is evident for the laponite containing systems. As Figure 5 shows, the average fiber diameter for the PWL solutions are generally higher than PW solutions with similar viscosities, and the diameters for the laponite containing systems do not correlate simply with the zero shear viscosities.

Normalized cumulative diameter frequencies have been plotted in Figures 6 and 7. Figure 6 shows the data for mixtures belonging to groups 1 and 3, and Figure 7 shows the same for groups 2, 4, and 5. In all cases, as laponite was added or increased, the zero shear viscosity in these groups increased.[37] However, the change in the distribution of diameter in groups 1 and 3 was different from groups 2, 4, and 5. In the case of groups 1 and 3, as the laponite content increased, the distribution shifted toward larger diameter values, i.e. almost all the fibers formed had a larger diameter than the sample(s) in the same group having lesser laponite content. This is consistent with the observation that the fiber diameter increases with the zero shear viscosity of the spinning solution. However, in the case of

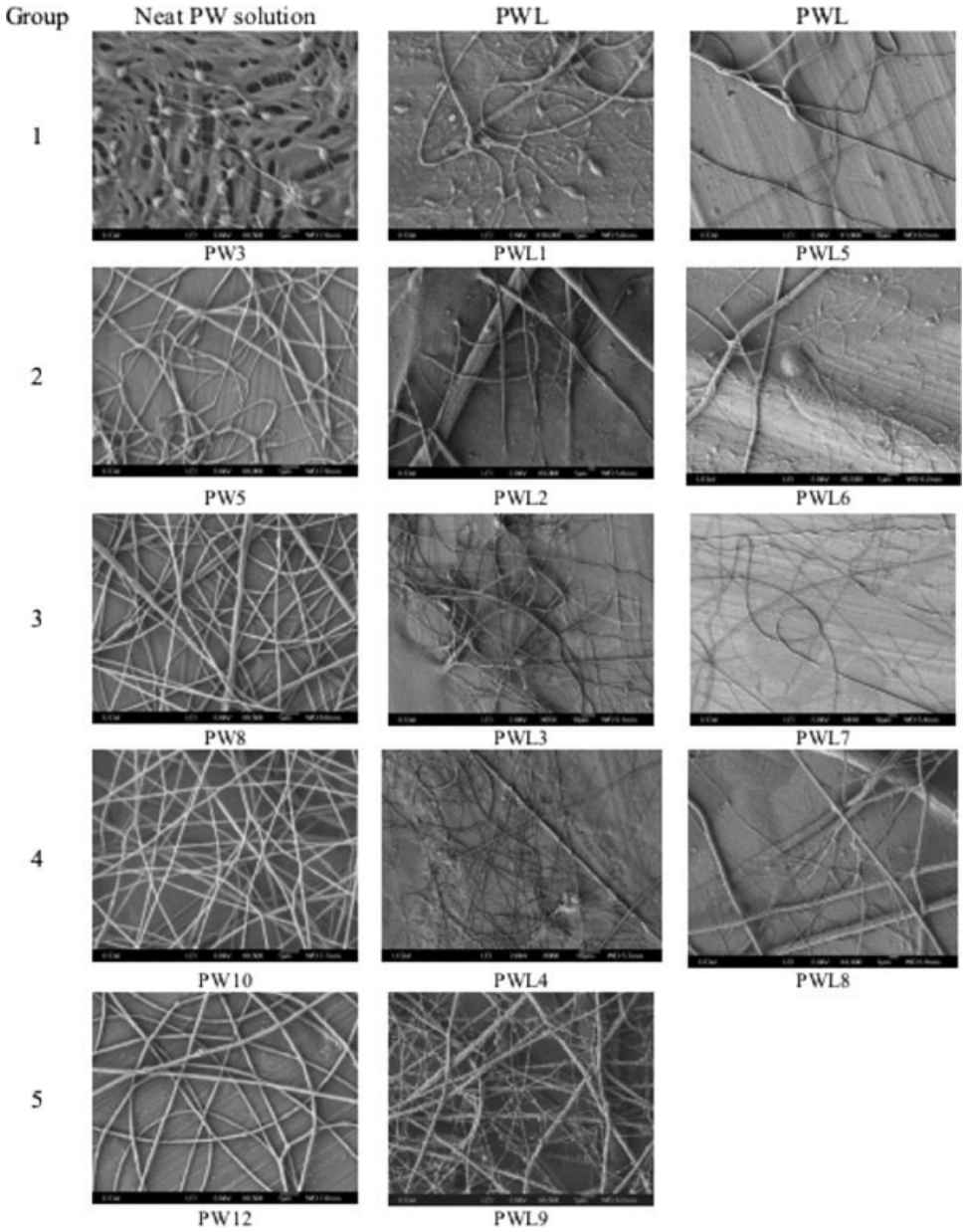

Figure 3. SEM micrographs of neat and laponite containing aqueous PEO solutions.

groups 2, 4, and 5, increasing the laponite concentration resulted in the formation of fibers with both greater and smaller diameters than the corresponding PW solutions. For example, PWL2 and PWL6 belong to group 2 with PWL6 containing a higher laponite content and yet a majority of fibers formed are of lesser diameters than those formed from PWL2, despite the increasing spinning solution viscosity with laponite addition. Similarly, for group 4, the addition of laponite results in many fibers smaller than those observed in the corresponding PW solutions.

RESULTS

Figure 4 compares the fiber diameters for PEO fibers versus spinning solution zero shear viscosity at two different electric fields ($E = 0.7$ kV/cm for Fong et al.[25] vs. 1.54 kV/cm) to the polyester fibers spun by McKee et al.[27] As seen, at fixed

Table 3. Spinning Solution Properties[37] and Resultant Fiber Diameters

Solution	Zero-Shear Viscosity (Pa s)	Conductivity (mS/cm)	Average Fiber Diameter (nm)	Standard Deviation in Diameter (nm)
PW3	0.18	0.078	84	24
PW5	0.91	0.101	133	32
PW8	2.65	0.108	153	24
PW10	6.44	0.118	178	52
PW12	15.6	0.128	191	28
PWL1	0.85	0.396	116	151
PWL2	1.93	0.331	800	720
PWL3	3.02	0.260	680	495
PWL4	7.37	0.191	375	284
PWL5	4.54	0.531	432	503
PWL6	4.46	0.446	519	488
PWL7	5.72	0.406	1166	621
PWL8	10.0	0.334	168	273
PWL9	17.5	0.247	144	140

solution viscosity, the diameter of the polyester fibers spun at $E = 0.75$ kV/cm are significantly larger than those spun from PEO at comparable field strength. Further, comparing the PEO fibers spun from solutions with the same viscosity shows a dependence on electric field strength. These results show that fiber diameter is not simply a function of spinning solution zero shear viscosity.

Consequently, although shear viscosity can be correlated to electrospinning performance for a single spinning solution containing only polymer, other solution properties and processing conditions, such as dielectric constant, surface tension, extensional properties, and solvent volatility may have a significant impact on final fiber size and fiber size distributions. Helgeson and Wagner[39] demonstrates a universal correlation between two parameters derived from dimensional analysis of electrospinning

$$Bh = \frac{2\bar{\varepsilon}^2\Phi_0^2}{K\eta_0 L^2},\ Oh = \frac{\eta_0}{(\rho\gamma R)^{1/2}}$$

where Bh is a ratio of electrostatic and electroviscous stresses, and Oh, the Ohnesorge number, relates viscous to inertial and surface forces. The Ohnesorge number has been shown[40] to govern capillary stability in free surface flows of electrified jets. These two dimensionless groups depend on the dielectric permittivity of air ($\varepsilon = 8.85 \times 10^{-12}$ C^2/N m), the applied voltage (Φ_0), the collector to tip distance (L), and the bead-free fiber diameter (R), as well as the spinning solution's conductivity (K), density (ρ), zero-shear viscosity (η_0), and surface tension (γ). Upon reducing electrospinning data from multiple sources using the dimensionless groups, an inverse correlation between Oh and Bh was observed, such that $Oh \sim 1/Bh$. Thus, the product of the two groups is approximately constant. Multiplying Bh and Oh as defined above yields a result that does not contain η_0, suggesting that the fiber size is, at best only weakly dependent on the zero-shear viscosity. Additionally, deviations from this scaling at low Oh can be explained in terms of capillary breakup of the

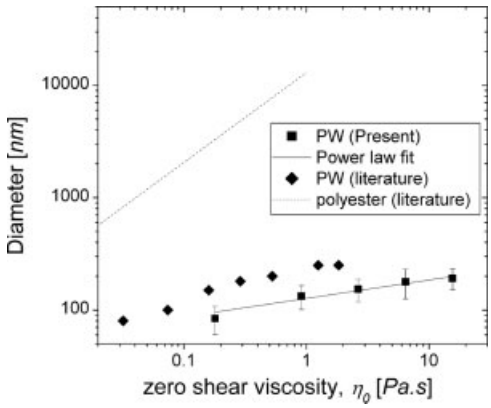

Figure 4. Dependence of the diameter of electrospun fibers of neat polymer solutions with the zero shear viscosity of the spun solutions: (■) PW solutions (present work) with electric field, $E = 1.54$ kV/cm; (◆◆) PW solutions at $E = 0.7$ kV/cm (Ref. 25); (– – –) the diameter correlation obtained for polyesters at $E = 0.75$ kV/cm (Ref. 27).

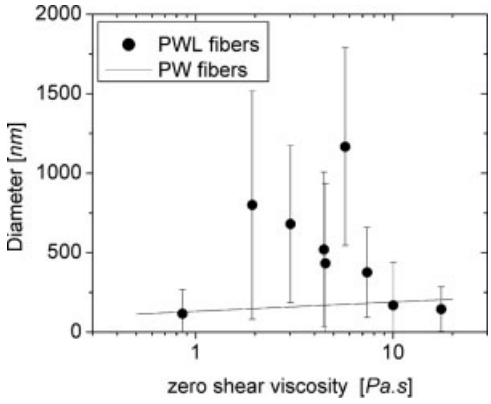

Figure 5. Diameter of electrospun fibers of laponite-filled aqueous PEO solutions compared to that for PW solutions.

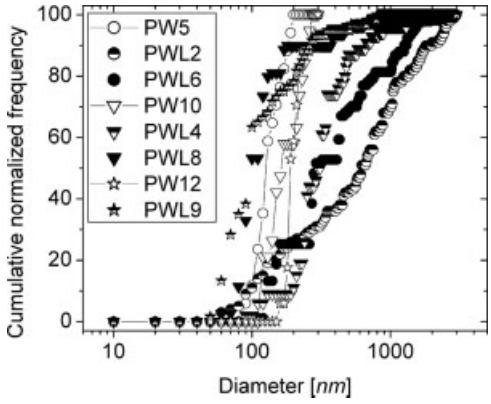

Figure 7. Diameter distribution of electrospun fibers belonging to groups 2, 4, and 5.

electrospinning jet resulting in beaded fibers.[39] Calculations of *Bh* and *Oh* for the neat PEO fibers presented here and the results presented by McKee et al.[27] and Fong et al.[25] are shown in Figure 8. The agreement between the three data sets when represented in this dimensionless form is very good even though the systems were spun in different laboratories with significant variations in PEO concentrations and spinning conditions. This analysis demonstrates that shear viscosity is not a relevant variable for correlating final fiber diameter.

If shear viscosity is not directly relevant to determining the final fiber diameter, the question remains as to why an apparent correlation can be obtained over limited and specific experimental results. As jet formation in electrospinning is primarily an elongational flow, the fiber diameter may be more fundamentally related to the elongational viscosity. Since the elongational viscosity is related to the shear viscosity by the Trouton ratio, which is the ratio of the elongational to the shear viscosity, correlations of electrospinning behavior with the shear viscosity are appropriate only if the Trouton ratio remains constant over the rates of extension experienced during electrospinning. The elongational rheology of aqueous PEO solutions has been studied extensively by Muller and coworkers,[41,42] who observed strong strain hardening (extensional thickening) at moderate to high extension rates due to a coil-stretch transition in the polymer chains. Since typical shear-thinning behavior is observed in the PEO and PEO–

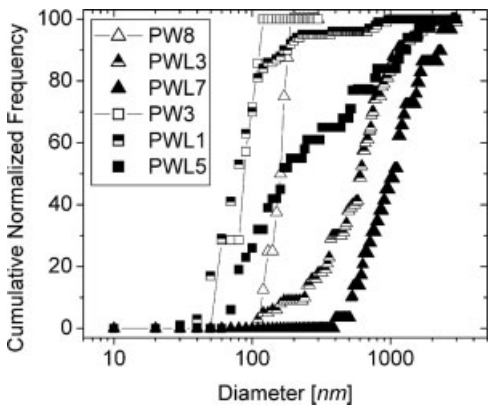

Figure 6. Diameter distribution of electrospun fibers belonging to groups 1 and 3. (The line + symbol representation of PW3 and PWL1 is to indicate the formation of beads on their electrospun fibers.)

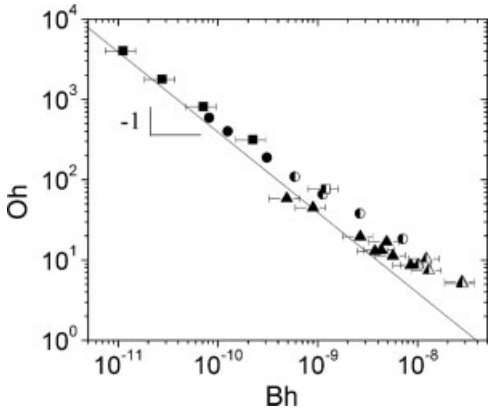

Figure 8. Correlation of electrospinning data using dimensional analysis for neat PEO solutions presented in this (■) and other[27] work (●), and for fibers spun from polyester solutions[1] (▲). Half-filled points represent fibers in which significant beading was reported.

laponite systems,[37] it is expected that the Trouton ratio will vary with the electrospinning conditions. This may explain the very weak dependence of fiber diameter on the zero-shear viscosity of the PW solutions, a result which may extend to a variety of polymer solutions and melts exhibiting extensional thickening.

Shenoy et al.[26] reviewed the concept that there is a transition from polymer beads to continuous fibers upon reaching a sufficient polymer chain entanglement density. However, as shown here, once this entanglement density has been reached and there is sufficient viscoelasticity and/or elongational viscosity to prevent bead formation, the final fiber diameter is nearly independent of the spinning solution's viscosity. The PEO solutions studied here and by others were well above the critical entanglement concentration and exhibited measurable viscoelasticity. This might help explain the significantly stronger dependence on viscosity reported for the polyester system by McKee et al.,[27] as their solutions were viscous, but Newtonian without measurable viscoelasticity. It is plausible that the dependence of fiber size on solution viscosity reported by McKee et al.[27] is a consequence of sensitivity to another solution property, such as surface tension and/or electrical conductivity, which varies systematically along with solution viscosity. This has been the subject of further investigation.[39]

Turning to the main topic of the effects of added nanoparticles on the fiber morphology and electrospinning process, the study, by Drew et al.,[29] of the effects of added TiO_2 particles on the properties of electrospun PEO fibers ($M_w = 3 \times 10^5$ g/mol) concluded that particle addition to the spinning solution to build viscosity was effective in producing electrospun fibers. Further, they report that above a minimum concentration, the presence of particles no longer affects fiber diameter. These conclusions are not supported by the work reported here on aqueous PEO–laponite solutions, suggesting that particle addition has influences on the solution's electrical properties and surface tension that are more significant than effects on the shear viscosity. As discussed in our previous work,[37] the addition of laponite builds viscosity through polymer adsorption and bridging. The interactions of PEO and laponite in water are rich and, in different compositions, lead to a variety of highly nonlinear materials such as "shake gels",[43] which exhibit significant strain hardening. Model calculations[44] demonstrate that strain hardening leads to thicker fibers. Thus, the addition of dispersed nanoparticles may significantly affect the elongational viscosity, and hence, the fiber diameters, and the effect will be specific to details of the polymer–particle interactions. Further exploration of this requires accurate, reliable measurements of the transient elongational viscosities at rates comparable to those observed during electrospinning.

Note that addition of nanoclay particles to a PEO solution leads to a significant broadening in the fiber size distribution. A key factor in rationalizing some of the differences between the two studies may be the state of dispersion of the nanoparticles in the PEO solutions. In particular, Drew et al.[29] report significant beading in the presence of the TiO_2 particles, which they attribute to particle aggregation in the spinning solution. The dimensional analysis (shown in Fig. 8) shows that the results of Drew et al.[29] were for solutions at low Ohnesorge number, such that beading may have been due to capillary breakup rather than particle aggregation. The particles used by Drew et al.[29] were 21 nm in diameter, which compare well in size with the disc-shaped laponite particles, which are 30 nm in diameter and 1–5 nm in thickness. Here, however, the nanoclay dispersions are well dispersed and do not show evidence of aggregation in fibers or significant bead formation. Further, the laponite–PEO solutions exhibit sufficient viscoelasticity, and sufficiently high Ohnesorge number, to avoid beading.

There are additional factors that might contribute to the increase in standard deviation in fiber diameter for the solutions containing nanoclay. A large degree of splaying[19,24] is evident in the SEM micrographs of electrospun PWL solutions. The addition of nanoclay (which is charged) and its counterions[45] increases the surface charge density of the solution, which is known to result in splaying through electrohydrodynamic instabilities that are alleviated by lowering the surface charge density through surface generation.[18] The data in Table 3 show that solutions with increased conductivity display a larger deviation in the electrospun fiber diameter when normalized by the average diameter. Thus, splaying can be traced to the increased solution charge density with increasing laponite content of the electrospinning solutions.

In conclusion, we observe a weak increase of fiber diameter with the spinning solution's zero shear viscosity for concentrated PEO–water

solutions, but view this as an artifact of more a more fundamental dependence of the electrospun fiber morphology on the spinning solutions elongational viscosity and electrical properties. Comparison with the literature[27] shows that such simplistic correlations with viscosity are, at best, specific to the polymer solution. Rather, a dimensionless scaling proposed by Helgeson and Wagner[39] is shown to provide a unifying description of the results for neat spinning solutions. Further, we find that although the addition of dispersed, model nanoclay particles to model PEO–water solutions leads to solutions with comparable linear viscoelastic properties,[37] the fibers formed show much broader distributions in diameter than expected based on the spinning solution's zero shear viscosity. Splaying is evident for the nanoclay containing solutions, which is attributed to the increase in charge density due to the nanoclay and associated counterions. Comparison to reports in the literature suggests that good particle dispersion and stability in solutions are important in producing fibers without beading. As demonstrated here, controlling the electrospun fiber mat morphology upon incorporating nanoparticles requires more than just consideration of the effects of the nanoparticles on the spinning solution's shear viscosity and conductivity.

Funding for this project was provided by the National Science Foundation (DMR-0210223). V. Krikorian is acknowledged for assistance with the electrospinning experiments, as well as Dr. Chaoying Ni and Frank Kriss for use of the W.M. Keck Electron Microscopy Facility. Dr. Joe Deitzel is acknowledged for useful conversations during the course of this work.

NOMENCLATURE

PEO	poly(ethylene oxide)
PW	PEO–water solution
PWL	PEO–water–laponite mixture
P	wt. % PEO in PWL mixture
L	wt. % laponite in PWL mixture
η_0	zero shear viscosity (Pa s)
D	diameter (nm)
ω	angular frequency (rad/s)
G'	storage modulus (Pa)
G''	loss modulus (Pa)
a_T	horizontal time–temperature shift factor
b_T	vertical time–temperature shift factor
a_c	horizontal time–concentration shift factor
b_c	vertical time–concentration shift factor

REFERENCES AND NOTES

1. Buer, A.; Ugbolue, S. C.; Warner, S. B. Text Res J 2001, 71, 323.
2. Hohman, M. M.; Shin, M.; Rutledge, G.; Brenner, M. P. Phys Fluids 2001, 13, 2201.
3. Hohman, M. M.; Shin, M.; Rutledge, G.; Brenner, M. P. Phys Fluids 2001, 13, 2221.
4. Huang, Z. M.; Zhang, Y. Z.; Kotaki, M.; Ramakrishna, S. Compos Sci Technol 2003, 63, 2223.
5. Jayaraman, K.; Kotaki, M.; Zhang, Y. Z.; Mo, X. M.; Ramakrishna, S. J Nanosci Nanotechnol 2004, 4, 52.
6. Reneker, D. H. Abstr Pap Am Chem Soc 2003, 225, U282.
7. Caruso, R. A.; Schattka, J. H.; Greiner, A. Adv Mater 2001, 13, 1577.
8. Doshi, J.; Reneker, D. H. J Electrostatics 1995, 35, 151.
9. Guan, H. Y.; Shao, C. L.; Liu, Y. C.; Yu, N.; Yang, X. H. Solid State Commun 2004, 131, 107.
10. Jia, H. F.; Zhu, G. Y.; Vugrinovich, B.; Kataphinan, W.; Reneker, D. H.; Wang, P. Biotechnol Prog 2002, 18, 1027.
11. Kataphinan, W.; Reneker, D. H.; Teye-Mensah, R.; Ramsier, R.; Edward, E. A.; Smith, D. J. Abstr Pap Am Chem Soc 2003, 225, U686.
12. Khil, M. S.; Bhattarai, S. R.; Kim, H. Y.; Kim, S. Z.; Lee, K. H. J Biomed Mater Res B Appl Biomater 2005, 72, 117.
13. Krauthauser, C.; Deitzel, J. M.; Wetzel, E. D.; O'Brien, D. Abstr Pap Am Chem Soc 2003, 226, U442.
14. Shields, K. J.; Beckman, M. J.; Bowlin, G. L.; Wayne, J. S. Tissue Eng 2004, 10, 1510.
15. Viswanathamurthi, P.; Bhattarai, N.; Kim, H. Y.; Khil, M. S.; Lee, D. R.; Suh, E. K. J Chem Phys 2004, 121, 441.
16. Zhang, G.; Kataphinan, W.; Teye-Mensah, R.; Katta, P.; Khatri, L.; Evans, E. A.; Chase, G. G.; Ramsier, R. D.; Reneker, D. H. Mater Sci Eng B: Solid State Mater Adv Technol 2005, 116, 353.
17. Casper, C. L.; Stephens, J. S.; Tassi, N. G.; Chase, D. B.; Rabolt, J. F. Macromolecules 2004, 37, 573.
18. Deitzel, J. M.; Kleinmeyer, J.; Harris, D.; Tan, N. C. B. Polymer 2001, 42, 261.
19. Deitzel, J. M.; Kleinmeyer, J. D.; Hirvonen, J. K.; Tan, N. C. B. Polymer 2001, 42, 8163.
20. Fridrikh, S. V.; Yu, J. H.; Brenner, M. P.; Rutledge, G. C. Phys Rev Lett 2003, 90, 144502.
21. Megelski, S.; Stephens, J. S.; Chase, D. B.; Rabolt, J. F. Macromolecules 2002, 35, 8456.
22. Shin, Y. M.; Hohman, M. M.; Brenner, M. P.; Rutledge, G. C. Polymer 2001, 42, 9955.
23. Shin, Y. M.; Hohman, M. M.; Brenner, M. P.; Rutledge, G. C. Appl Phys Lett 2001, 78, 1149.
24. Yarin, A. L.; Koombhongse, S.; Reneker, D. H. J Appl Phys 2001, 89, 3018.

25. Fong, H.; Chun, I.; Reneker, D. H. Polymer 1999, 40, 4585.
26. Shenoy, S. L.; Bates, W. D.; Frisch, H. L.; Wnek, G. E. Polymer 2005, 46, 3372.
27. McKee, M. G.; Wilkes, G. L.; Colby, R. H.; Long, T. E. Macromolecules 2004, 37, 1760.
28. McKee, M. G.; Elkins, C. L.; Long, T. E. Polymer 2004, 45, 8705.
29. Drew, C.; Wang, X. Y.; Samuelson, L. A.; Kumar, J. J Macromol Sci Pure Appl Chem 2003, 40, 1415.
30. Krikorian, V.; Casper, C.; Rabolt, J.; Pochan, D. J. Abstr Pap Am Chem Soc 2004, 227, U474.
31. Salalha, W.; Dror, Y.; Khalfin, R. L.; Cohen, Y.; Yarin, A. L.; Zussman, E. Langmuir 2004, 20, 9852.
32. Ye, H. H.; Lam, H.; Titchenal, N.; Gogotsi, Y.; Ko, F. Appl Phys Lett 2004, 85, 1775.
33. Devanand, K.; Selser, J. C. Macromolecules 1991, 24, 5943.
34. Hammouda, B.; Ho, D.; Kline, S. Macromolecules 2002, 35, 8578.
35. Hammouda, B.; Ho, D. L.; Kline, S. Macromolecules 2004, 37, 6932.
36. Ho, D. L.; Hammouda, B.; Kline, S. R. J Polym Sci Part B: Polym Phys 2003, 41, 135.
37. Daga, V.; Wagner, N. J. Rheol Acta, in press, 2006.
38. Mongondry, P.; Nicolai, T.; Tassin, J. F. J Colloid Interface Sci 2004, 275, 191.
39. Helgeson, M. E.; Wagner, N. J. Nano Lett, in preparation, 2006.
40. Lopez-Herrera, J. M.; Ganan-Calvo, A. M. J Fluid Mech 2004, 501, 303.
41. Chow, A.; Keller, A.; Muller, A. J.; Odell, J. A. Macromolecules 1988, 21, 250.
42. Muller, A. J.; Odell, J. A.; Keller, A. J Non-Newtonian Fluid Mech 1988, 30, 99.
43. Pozzo, D. C.; Walker, L. M. Colloid Surf Physicochem Eng Aspect 2004, 240, 187.
44. Feng, J. J. J Non-Newtonian Fluid Mech 2003, 116, 55.
45. Willenbacher, N.; Hanciogullari, H.; Wagner, H. G. Chem Eng Technol 1997, 20, 557.